# In Vitro Biosynthesis of Violacein from L-Tryptophan by the Enzymes VioA−E from *Chromobacterium violaceum*†

Carl J. Balibar and Christopher T. Walsh*

*Department of Biological Chemistry & Molecular Pharmacology, Harvard Medical School, 240 Longwood Avenue, Boston, Massachusetts 02115*

*Received September 26, 2006; Revised Manuscript Received November 3, 2006*

ABSTRACT: The purple chromobacterial pigment violacein arises by enzymatic oxidation and coupling of two molecules of L-tryptophan to give a rearranged pyrrolidone-containing scaffold in the final pigment. We have purified five contiguously encoded proteins VioA−E after expression in *Escherichia coli* and demonstrate the full 14-electron oxidation pathway to yield the final chromophore. The flavoenzyme VioA and the heme protein VioB work in conjunction to oxidize and dimerize L-tryptophan to a nascent product that can default to the off pathway metabolite chromopyrrolic acid. In the presence of VioE, the intermediate instead undergoes on-pathway [1,2] indole rearrangement to prodeoxyviolacein. The last two enzymes in the pathway are flavin-dependent oxygenases, VioC and VioD, that act sequentially. VioD hydroxylates one indole ring at the 5-position to yield proviolacein, and VioC then acts on the other indole ring at the 2-position to create the oxindole and complete violacein formation.

The amino acid tryptophan is shunted down oxidative secondary metabolic pathways in a variety of microbes that produce indole-containing natural products. This includes the biosynthetic pathways to rebeccamycin (**1**) and staurosporine (**2**) (Figure 1) where oxidative dimerization creates the fused six-ring indolocarbazole scaffold of these DNA-binding and protein kinase inhibitors, respectively (*1*, *2*). A variant of such oxidative dimerization occurs in *Chromobacterium violaceum* to yield the violet pigment known as violacein (**8**) (*3*, *4*). Violacein has been known since 1882 (*5*) as a water-insoluble blue-black dye of microbial origin in soils and aqueous environments of the tropics where its production may shield microbial producers against UV irradiation (*6*). Since its initial discovery, violacein has been shown to possess a wide range of biological effects, including antibacterial (*7*−*9*), antiviral (*8*, *10*, *11*), antitumorigenic (*8*, *12*−*17*), antitrypanosomatid (*8*, *18*−*21*), and antiulcerogenic activities (*22*).

The structure of **8** is composed of three structural units, a 5-hydroxyindole and a 2-oxindole connected to the 5- and 3-positions of a 2-pyrrolidone core, respectively (*4*, *23*). The entirety of the carbon, hydrogen, and nitrogen skeleton of violacein has been shown to derive from two molecules of L-tryptophan, whereas the three oxygen atoms originate from molecular oxygen (*4*, *24*). In addition to the pyrrole nucleus of violacein, which is found in many interesting biologically relevant natural products (*25*), the most fascinating aspect in the biosynthesis of violacein is an intramolecular 1,2-shift of the 5-hydroxyindole half of the molecule (*4*, *26*). Such 1,2-shifts are extremely rare in metabolism and have been observed for hydrogen atoms during the hydroxylation of aromatic rings (NIH shift) (*27*), migration of a phenyl substituent in conversion of flavanone to isoflavone (*28*), and in rearrangement of (*R*)-littorine to (*S*)-hyoscyamine (*29*). The latter two aromatic shifts are carried out by cytochrome P450 enzymes.

In recent years, various gene clusters responsible for violacein production have been isolated, sequenced, and heterologously expressed in *Escherichia coli* and other bacteria (*30*−*32*). All have been shown to contain four contiguous genes, VioA−D, which were deemed sufficient for violacein production. VioC and VioD were annotated as monooxygenases, and through genetic knockouts were determined to be responsible for oxidation at the 2- and 5-positions of the two indoles, respectively (*30*). Less is known about the VioA and VioB gene products, mainly because disruption of either of these genes leads to complete loss of pigment production (*30*, *31*). VioA by sequence similarity was annotated as a tryptophan 2-monooxygenase, whereas VioB was annotated as a polyketide synthase, albeit with extremely low sequence similarity (*30*).

Our examination of the VioB primary sequence reveals that it in fact resembles RebD, StaD, and InkD, enzymes involved in the biosynthesis of the indolocarbazoles **1** (*33*), **2** (*34*), and K-252a (**3**) (*35*), respectively. We have recently characterized RebD as an enzyme responsible for converting the imine of indole-3-pyruvate (IPA), generated by the L-Trp amino acid oxidase RebO, into chromopyrrolic acid (CPA)[1] (**4**) in the rebeccamycin pathway (*36*). The RebOD pair is more than likely analogous to the VioAB pair at the start of the violacein pathway for tryptophan oxidation and dimerization. This is supported by the fact that certain mutants of *C. violaceum* no longer produce **8** but instead make CPA (*37*). The connectivity in violacein differs from rebeccamycin

†We gratefully acknowledge NIH GM 20011 (C.T.W.) and a Department of Defense National Defense Science and Engineering Graduate Fellowship (C.J.B.).

* To whom correspondence should be addressed. E-mail: christopher_walsh@hms.harvard.edu. Phone: (617) 432-1715. Fax: (617) 738-0438.

10.1021/bi061998z CCC: $33.50 
Published on Web 12/19/2006

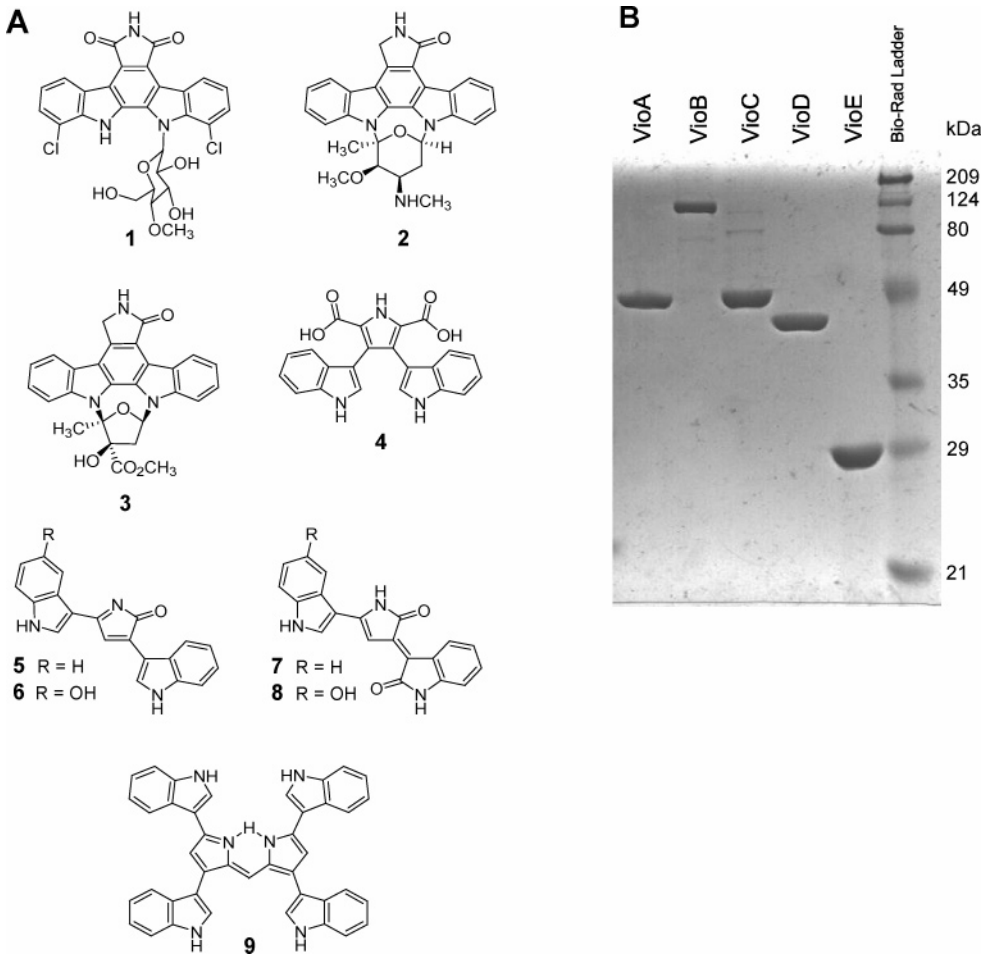


FIGURE 1: (A) Structures of rebeccamycin (**1**), staurosporine (**2**), K-252a (**3**), chromopyrrolic acid (CPA) (**4**), prodeoxyviolacein (**5**), proviolacein (**6**), deoxyviolacein (**7**), violacein (**8**), and deoxychromoviridans (**9**). (B) 12% SDS−PAGE gel of the five proteins from the violacein gene cluster.

and staurosporine by the aforementioned 1,2 (H, indole) shift (*4*, *26*) that has occurred at some stage in its assembly, most likely during formation of prodeoxyviolacein (**5**) (*38*).

There are several outstanding questions regarding the biosynthesis of violacein. On the basis of feeding experiments, it has been proposed that 5-hydroxy-L-tryptophan serves as a precursor for violacein biosynthesis (*6*, *39*); however, contradictory results also have been observed in which 5-hydroxy-L-tryptophan fed to *C. violaceum* was not efficiently incorporated into the final violacein molecule (*3*). It is possible that VioD hydroxylates violacein at a late stage in biosynthesis, especially since deoxyviolacein (**7**) is a compound known to be produced by *C. violaceum* along with fully oxidized violacein. If this is the case, then it has been unknown whether VioC or VioD performs hydroxylation first, since all four combinations of pro- and/or deoxyviolacein can be observed (*38*). Absolutely nothing is known about the enzymatic reaction that leads to formation of the pyrrolidone nucleus, nor the factors responsible for controlling the 1,2-shift of the indole. If VioAB in fact mirror the activity of RebOD, then it is unclear how the system is able to divert intermediates away from CPA, since CPA is known not to be on the pathway to violacein (*37*). A very recent in vivo study by Sachez et al. has shed some light on these questions (*40*). In particular, a fifth gene, VioE, was found to be important for formation of prodeoxyviolacein, and VioC and VioD were found to act after prodeoxyviolacein formation.

Herein we reconstitute the entire violacein pathway in vitro. We demonstrate that L-tryptophan, and not 5-hydroxy-L-tryptophan, is the sole precursor to violacein. VioB is responsible for the oxidative coupling of two molecules of IPA imine generated by VioA for formation of the pyrrole core, but a fifth gene, VioE, is responsible for the indole shift that results in formation of **5** rather than **4**. Formation of **8** then proceeds by the sequential action of VioD and VioC. Our work independently confirms and elaborates on recent in vivo results (*40*), allowing detailed enzymatic information to be described.

## EXPERIMENTAL PROCEDURES

*Materials and General Methods.* Standard recombinant DNA, molecular cloning, and microbiological procedures were performed as described (*41*). Competent Top10 and

[1] Abbreviations: CPA, chromopyrrolic acid; IPA, indole-3-pyruvic acid; PCR, polymerase chain reaction; IPTG, isopropyl $\beta$-D-1-thiogalactopyranoside; HPLC, high-performance liquid chromatography; LCMS, liquid chromatography mass spectrometry; SDS−PAGE, sodium dodecyl sulfate−polyacrylamide gel electrophoresis; DTT, dithiothreitol; BSA, bovine serum albumin; TCA, trichloroacetic acid; TFA, trifluoroacetic acid; 5OH-L-Trp, 5-hydroxy-L-tryptophan; ICP-MS, inductively coupled plasma mass spectrometry; NAD(P)H, nicotinamide adenine dinucleotide (phosphate), reduced form; FAD, flavin adenine dinucleotide; FMN, flavin mononucleotide; HRP, horseradish peroxidase; THF, tetrahydrofolate.

BL21 (DE3) *E. coli* strains were from Invitrogen. Oligonucleotide primers were from Integrated DNA Technologies. Phusion DNA polymerase, restriction enzymes, and T4 DNA ligase were from New England Biolabs. Plasmids pET24b, pET21b, and pETBlue-2 were from Novagen. DNA sequencing to verify PCR fidelity was performed on double-stranded DNA by the Molecular Biology Core Facilities of the Dana Farber Cancer Institute (Boston, MA). Plasmid DNA preparation was performed using the Qiaprep kit from Qiagen. Gel extraction of DNA fragments as well as restriction endonuclease cleanup were done using the GFX kit from GE Healthcare. Ni-NTA Superflow resin was from Qiagen. FPLC purification of proteins was performed using a HiLoad 26/60 Superdex 200 preparative grade column run on a P-920 pump equipped with a UPC-900 detector and a Frac-950 fraction collector (GE Healthcare). SDS−PAGE gels were from BioRad. Protein samples were concentrated using a 10KMWCO Amicon Ultra device from Millipore and final protein concentrations were calculated using either the method of Bradford (*42*), with BSA as a standard (VioA, VioB, VioC, and VioD) or the protein's absorbance at 280 nm and the predicted molar extinction coefficient (VioE). FAD, FMN, hematin, NAD(P)H, $\delta$-aminolevulinic acid, L-tryptophan, and 5-hydroxy-L-tryptophan were purchased from Sigma.

Preparative HPLC was performed on a Beckman Coulter System Gold instrument with a Vydac Proteins and Peptides C18 column (10 $\mu$m, 22 × 250 mm). RadioHPLC was performed on a Beckman Coulter System Gold instrument equipped with a $\beta$-Ram module 3 radioisotope detector (IN/US Systems). LCMS identification was carried out on a Shimadzu LCMS-QP8000α equipped with two LC-10AD*VP* liquid chromatography pump modules, a SPD-10AV*VP* UV−vis detector, a SIL-10AD*VP* autosampler module, and a Vydac C18 Mass Spec column (5 $\mu$M, 2.1 × 250 mm).

*Cloning, Expression, and Purification of Vio Proteins.* All constructs were obtained from PCR amplification of genomic DNA from *C. violaceum* ATCC 12472. This template was amplified using the following primers (underlined: restriction site): VioA: 5′-AGGACATTCCATATGAAGCATTCTTCCG-ATATCTGC-3′ and 5′-CGGCCGGACCTCGAGCGCGGC-GATGCGCTGCAGCAG-3′; VioB: 5′-TTCGGGAAA-CATATGAGCATTCTGGATTTTCCACGC-3′ and 5′-GCT-CTTTTCCTCGAGGGCCTCTCTAGAAAGCTTTCC-3′; VioC: 5′-GAGAGGCCTCATATGAAAAGAGCAATCAT-AGTCGGA-3′ and 5′-CAGAATCTCTCGAGGTTGAC-CCTCCCTATCTTGTAC-3′; VioD: 5′-GAGGGTCAA-CATATGAAGATTCTGGTCATCGGCGCG-3′ and 5′-CAT-GCGGCCCTCGAGGCGTTGCAGCGCGTAGCGCAG-3′, VioE: 5′-GAGGAGGCCATATGGAAAACCGGGA-ACCGCCGCTG-3′ and 5′-CCGATCCAGCTCGAGGCGCT-TGGCGGCGAAGACGGC-3′. All PCR products were digested with *Nde*I/*Xho*I and ligated into a similarly digested pET24b vector.

The described expression plasmids were transformed into *E. coli* BL21 (DE3) competent cells. VioA−D were grown at 15 °C and VioE was grown at 25 °C in Luria−Bertani media with 40 $\mu$g/mL kanamycin (supplemented with 1 mM $\delta$-aminolevulinic acid and 40 $\mu$M ammonium iron sulfate for VioB) to an $OD_{600}$ of 0.7 when the culture was induced with 100 $\mu$M IPTG and then grown for an additional 24 h. The cells were harvested by centrifugation at 4000*g* for 16 min. Cell pellets from 6 L of fresh culture were resuspended in 30 mL of lysis buffer (25 mM Tris, pH 8.0, 500 mM NaCl) and then lysed with two passes on an Emulsiflex-C5 cell disruptor (Avestin). The lysate was cleared by ultracentrifugation at 95000*g* for 35 min and then transferred to 1.2 mL of Ni-NTA resin for incubation at 4 °C for 1.5 h. The resin was then transferred to a column and the protein was eluted with an imidazole gradient using steps of 25 mL of 0 and 5 mM imidazole, 15 mL of 25 and 200 mM imidazole, and 10 mL of 500 mM imidazole mixed into lysis buffer (supplemented with 10% glycerol for VioC). Volumes were doubled for elution of VioB. For in vitro reconstitution (VioA, VioC, and VioD), protein still bound to the nickel column before the 5 mM imidazole elution step was incubated with 5 mL of 4 mM FAD for 1 h. After an SDS−PAGE gel was run to verify which fractions contained the protein, it was concentrated to 1.5 mL and subjected to gel filtration purification with a running buffer of 20 mM Tris, pH 8.4 and 50 mM NaCl (VioA, VioB, VioD), 20 mM Tris, pH 8.4, 50 mM NaCl, and 10% glycerol (VioC), or 20 mM Tris, pH 8, 50 mM NaCl, 2 mM $MgCl_2$, and 1 mM DTT (VioE). After confirming which fractions contained the protein of interest using SDS−PAGE, the resulting fractions were concentrated, supplemented with 10% glycerol, flash frozen in liquid nitrogen, and stored at −80 °C.

*Characterization of Cofactors Bound to Vio Enzymes.* The nature of the bound cofactor for VioA, VioC, and VioD was determined using analytical HPLC and UV−visible spectrophotometry. Protein samples that had not been subjected to the aforementioned reconstitution were denatured (100 °C for 20 min), precipitated, and then analyzed on a Phenomenex C18 5$\mu$ Luna column 250 × 4.6 mm using a gradient of 0−50% acetonitrile over 20 min, starting in 0.1% TFA in $H_2O$. Once it was determined that all three contained FAD from coelution with authentic standard, the flavin content of the solution was measured by UV−vis spectrophotometry using the known extinction coefficient of FAD ($\epsilon_{450}$ = 11 300 $M^{-1}$ $cm^{-1}$). The identity and content of the heme bound to VioB were determined by the pyridine hemochrome assay (*43*), and the iron content was measured using the Ferene S assay (*44*). Inductively coupled plasma mass spectrometry (ICP-MS) was performed by Elemental Research Inc. to detect the presence of nine metals in a sample of VioE (Ca, V, Mn, Fe, Co, Ni, Cu, Zn, Mo).

*Enzymatic Reactions on L-Tryptophan by VioA and VioD.* Assays to optimize pH for VioA oxidation of trytophan contained 1 $\mu$M VioA, 1 $\mu$M FAD, 75 mM buffer (HEPES for pH 7.5−8.0, Tris for pH 8.0−9.0, and glycine for pH 9.0−9.5), and 250 $\mu$M L-Trp. A total of 100 $\mu$L of reaction was quenched at various time points with 20 $\mu$L of 50% TCA and centrifuged to pellet the protein. The supernatant containing the product was analyzed by HPLC on a Vydac 250 × 4.6 mm C18 small pore column, using a gradient of 0−50% acetonitrile over 20 min starting in 0.1% TFA in $H_2O$, monitoring absorbance at 280 nm.

Assays to determine kinetic parameters for VioA oxidation by monitoring disappearance of substrate contained 1 $\mu$M VioA, 1 $\mu$M FAD, 75 mM glycine, pH 9.25, and various concentrations of L-Trp or 5OH-L-Trp. At desired time points, 100 $\mu$L of the reaction was quenched with 20 $\mu$L of 50% TCA and centrifuged to pellet the protein. The product was analyzed as described above. Assays to determine kinetic

parameters for VioA oxidation by monitoring production of peroxide contained 50 $\mu$M Amplex Ultra Red (Invitrogen), 10 units/mL horseradish peroxidase (Sigma), 25 mM glycine pH 9.0, 50 nM VioA, 50 nM FAD, and various concentrations of L-Trp or 5OH-L-Trp. The reaction was monitored constantly over 10 min spectrophotometrically at 568 nM.

Assays to determine whether VioD would hydroxylate L-tryptophan contained 1 $\mu$M VioD, 75 mM Tris pH 9.0, 100 $\mu$M L-Trp, 1 $\mu$M FAD, ± 200 $\mu$M NAD(P)H, ± 500 $\mu$M $CuSO_4$, ± 1 $\mu$M SsuE (*45*). Reactions were incubated at room temperature for 30 min and analyzed as described above for VioA.

Anaerobic reactions on VioA were performed in a Unilab glovebox (Mbraun, Stratham, NH) with oxygen levels maintained at or below 2 ppm. All reagents and solutions were degassed by bubbling argon for 10 min prior to their introduction into the glovebox, and then equilibrated overnight to remove residual traces of oxygen. VioA was deoxygenated by passing through Bio-Gel P6 DG desalting gel (Bio-Rad) in the glove box. Reactions contained 20 $\mu$M [$^{14}$C]-L-Trp (133 mCi/mmol) (Perkin-Elmer), 22.5 $\mu$M VioA, and 75 mM glycine pH 9.25. After 20 min, the 80 $\mu$L reaction was quenched with 16 $\mu$L of 50% TCA and centrifuged to pellet the protein. The product was analyzed by radioHPLC using a gradient of 0−50% acetonitrile over 20 min starting in 0.1% TFA in $H_2O$, monitoring $^{14}$C radioactive counts.

*$O_2$ Electrode Assay*. Oxygen production by VioB was assessed using a Hansatech D.W. oxygen electrode unit, based on a Clark-type oxygen electrode (*46*). The instrument was calibrated by measuring net oxygen consumption of 1.8 $\mu$M 2,3-dihydroxybiphenyl dioxygenase in the presence of 50, 100, and 150 $\mu$M 2,3-dihydroxybiphenyl (*47*). Rates of peroxide disproportionation by VioB were measured by reference to the calibration curve and compared to a standard of catalase.

*Genetic Analysis of the Violacein Cluster*. Genomic DNA from *C. violaceum* ATCC 12462 was digested with *Mlu*I and *Xho*I and run on a 1% agarose gel to isolate those fragments between 7 and 10 kbp. After gel extraction and purification, the fragments were ligated into a similarly digested pET24b vector and transformed into Top10 cells. After 36 h at 37 °C, two purple colonies appeared, which were determined to contain the violacein cluster by performing various digest screens on miniprepped DNA. This parental plasmid was named pVio. Deletion mutants of this plasmid were created by digesting with *Nco*I, *Bgl*II, *Pml*I, *EcoR*I, *Stu*I, *BstB*I, and *Bbv*CI, gel purifying the fragments, ligating, and transforming into Top10 cells. These plasmids—named pVioΔ*Nco*I, pVioΔ*Bgl*II, pVioΔ*Pml*I, pVioΔ*EcoR*I, pVioΔ*Stu*I, pVioΔ*BstB*I, and pVioΔ*Bbv*CI, respectively—were verified with various digest screens.

The violacein cluster was further cloned into pETBlue-2 to define its boundaries. pVio was digested with *Mlu*I/*Xho*I, *Mlu*I/*Asc*I, *Mlu*I/*Aat*II, *Sbf*I/*Xho*I, *Sbf*I/*Asc*I, and *Sbf*I/*Aat*II, run on a 1% agarose gel to isolate the proper inserts, ligated into a similarly digested pETBlue-2 vector, and transformed into Top10 cells. After 48 h of incubation at 37 °C, very small intensely colored colonies appeared for those four constructs that would produce violacein. The longer incubation time and smaller colony size is due to pETBlue-2 being a high copy number plasmid and violacein having antibiotic properties. These plasmids were named pVio2-*Mlu*I/*Xho*I, pVio2-*Mlu*I/*Asc*I, pVio2-*Mlu*I/*Aat*II, pVio2-*Sbf*I/*Xho*I, pVio2-*Sbf*I/*Asc*I, and pVio2-*Sbf*I/*Aat*II, respectively, and were verified by various digest screens.

For complementation experiments, the violacein cluster from pVioΔ*BbvC*I was digested with *Mlu*I/*Xho*I and ligated into pET21b yielding pVio21Δ*BstB*I. Additionally, the violacein cluster from pVio2-*Mlu*I/*Aat*II and pVio2-*Sbf*I/*Aat*II were digested with *Nhe*I/*Xho*I and ligated into pET21b yielding pVio21-*Mlu*I/*Aat*II and pVio21-*Sbf*I/*Aat*II. These three pVio21 plasmids were cotransformed with the expression plasmid for VioE, pVioE, described previously, into BL21 (DE3) cells yielding purple colonies in all three cases.

*Purification of Deoxychromoviridans.* A total of 8 L of Top10 cells expressing pVioΔ*BstB*I was grown for 3 days at 30 °C in Luria−Bertani media supplemented with 500 $\mu$M L-Trp, harvested by centrifugation at 4000*g*, and then extracted 4 times with 150 mL of boiling methanol. The resulting solution was evaporated to dryness, redissolved in a minimal volume of 6:1 dichloromethane/methanol, and loaded onto a silica gel column. Deoxychromoviridans (**9**) was eluted with the same 6:1 dichloromethane/methanol mobile phase. After the sample was evaporated to dryness, the solid was redissolved in DMSO and injected directly onto a preparative HPLC using a gradient of 20−100% acetonitrile over 45 min starting in 0.1% TFA in $H_2O$. The compound came off as a pure teal-colored peak, which was evaporated to dryness: 605.2 $[M + H]^+$ calculated, 605.1 observed. 600 MHz $^1$H NMR (DMSO-$d_6$) $\delta$ 7.18 (t, $J = 6.8$ Hz, 2H), 7.23 (t, $J = 7.0$ Hz, 2H), 7.32 (m, 4H), 7.41 (s, 2H), 7.46 (s, 1H), 7.49 (d, $J = 7.9$, 2H), 7.60 (d, $J = 9.0$, 2H), 7.63 (s, br, 2H), 7.95 (d, $J = 7.6$, 2H), 8.20 (s, br, 2H), 8.62 (s, br, 2H), 11.65 (s, br, 2H), 12.20 (s, br, 2H), 12.28 (s, br, 1H).

*Assays for Production of Prodeoxyviolacein.* 50 $\mu$L reactions contained 5 $\mu$M VioA, 5 $\mu$M VioB, 5 $\mu$M VioE, 50 units of catalase, 75 mM glycine pH 9.25, and 500 $\mu$M L-Trp as a starting point. Reagents were omitted or modified as noted. In the case in which RebD was used in place of VioB, the buffer was HEPPS pH 8.5. Reactions were quenched by addition of 20% DMSO (10 $\mu$L) and 200% methanol (100 $\mu$L), centrifuged at 13 000 rpm to pellet protein, and analyzed by analytical HPLC on a Phenomenex C18 5$\mu$ Luna column using a gradient of 20−74% acetonitrile over 36 min starting with 0.1% TFA in $H_2O$. Products were monitored at 280 or 590 nm.

*Assays for Hydroxylation by VioC and VioD.* The above starting reaction was incubated for 1.5 h, and then 5 $\mu$M VioC and/or 5 $\mu$M VioD were added with or without 5 mM NAD(P)H. Reactions were quenched by the aforementioned method. For reactions in which proviolacein or deoxyviolacein were the substrate, the above reaction was supplemented with 5 $\mu$M NAD(P)H and 5 $\mu$M VioD or VioC, respectively, After the sample was incubated for 2 h, to allow the reaction to go to completion, the reciprocal hydroxylase was added with an additional 5 $\mu$M NAD(P)H to assess its ability to act on a two-electron oxidized version of prodeoxyviolacein. All products were verified by comparison to known UV−vis spectra (*38*, *40*, *48*) and mass determined by LCMS (Figure 7A).

## RESULTS

*Purification and Characterization of VioA and VioD.* To address the question of whether 5-hydroxy-L-tryptophan is a precursor to violacein biosynthesis, we purified VioD, the proposed L-tryptophan 5-hydroxylase, and VioA, the proposed L-amino acid oxidase, to determine substrate specificity. VioA and VioD were cloned as C-terminal $His_6$-tagged proteins and expressed in *E. coli* at 15 °C, yielding approximately 25 mg/L of protein for each construct. The 48 kDa VioA and 42 kDa VioD proteins were purified to homogeneity using nickel-affinity chromatography and gel filtration in tandem (Figure 1B). Both the flavin dependent L-amino acid oxidase, VioA, and monooxygenase, VioD, purified with FAD as bound cofactor, as determined by analytical HPLC using authentic standards (data not shown). Using UV−vis spectroscopy, the FAD occupancy was determined to be 50% for VioA with or without reconstitution with exogenous FAD, whereas the percent occupancy increased from 23 to 72% for VioD after in vitro reconstitution.

VioD was tested for its ability to hydroxylate L-tryptophan. Incubations of VioD and NAD(P)H with L-tryptophan did not produce 5-hydroxy-L-tryptophan as determined by analytical HPLC with authentic 5OH-L-Trp standard. To address the possibility that VioD is a two-component monooxygenase, requiring an external reductase to generate reduced $FADH_2$, reactions were repeated with the FAD/FMN reductase SsuE (*45*) to generate reduced flavin in situ for direct use by VioD. Still, no formation of 5OH-L-Trp was observed. Finally, it had been reported that VioD may be a copper-dependent enzyme (*38*), so all experiments were repeated with the addition of $CuSO_4$. Again, no product was formed (data not shown).

With no activity observed for VioD, we sought to determine the kinetic parameters of VioA toward L-tryptophan and 5-hydroxy-L-tryptophan to ascertain which is the better substrate. In the L-amino acid oxidase reaction cycle, oxidized flavin reacts with (5OH)-L-Trp to generate the (5OH)-IPA imine and reduced flavin. The reduced flavin then reacts with molecular oxygen to form hydrogen peroxide and regenerate oxidized flavin. Because of the instability of the IPA product, kinetics of VioA amino acid oxidation were monitored either by the disappearance of L-Trp or 5OH-L-Trp by HPLC or by the generation of peroxide through a coupled peroxidase assay, which should be stoichiometric with product formation. Initial activity assays with VioA were performed at pH 7.5, the optimal pH for RebO, the L-Trp oxidase from the rebeccamycin system (*36*); however, slow turnover was observed. Since violacein and its precursors have pH indicator properties and are most intensely violet colored at higher pH, it was postulated that perhaps the violacein biosynthetic enzymes would be more active at higher pH. Therefore, before kinetics were performed, a pH profile for VioA activity was determined. VioA has optimal activity at pH 9.25, almost 2 pH units above that of RebO (data not shown).

Subsequently, Michaelis−Menten kinetic parameters were determined for VioA. The $k_{cat}$ and $K_M$ for L-tryptophan are $203 \pm 19$ min$^{-1}$ and $31 \pm 11$ $\mu$M, respectively, and the $k_{cat}$ and $K_M$ for 5-hydroxy-L-tryptophan are $174 \pm 13$ min$^{-1}$ and $165 \pm 30$ $\mu$M, respectively, as determined by monitoring

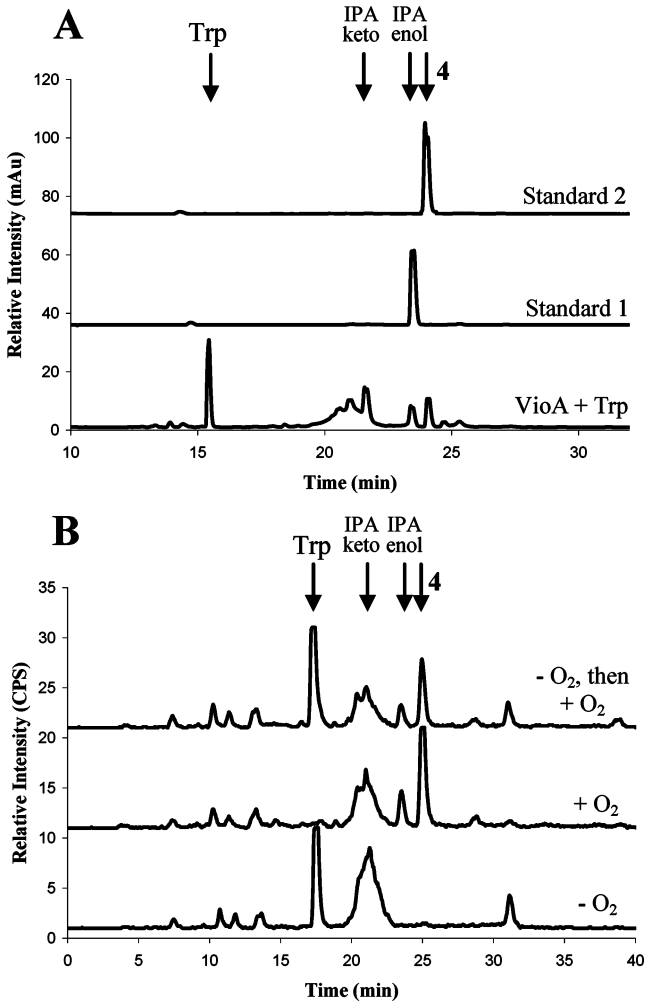


FIGURE 2: (A) HPLC trace of products formed upon incubation of 1 $\mu$M VioA with 250 $\mu$M L-Trp monitoring absorbance at 280 nm. Standard 1 is of indole-3-pyruvate (IPA), and standard 2 is of chromopyrrolic acid (CPA) (**4**). (B) HPLC trace of products formed upon incubation of 22.5 $\mu$M VioA with 20 $\mu$M L-Trp either anaerobically followed by direct injection on the HPLC ($-O_2$), aerobically ($+O_2$), or anaerobically followed by exposure to $O_2$ for 2 h after quenching ($-O_2$, then $+O_2$). Products were monitored by $^{14}C$ counts. The migration of IPA as two peaks has been observed previously (*36*) and is attributed to its keto and enol tautomers.

substrate disappearance. The kinetic parameters as determined by the tandem peroxidase assay were somewhat different, although they were consistent with tryptophan being the better substrate. There are several possibilities as to why the peroxidase assay did not completely correlate with the assay directly monitoring substrate utilization. Horseradish peroxidase (HRP) may not be fully active at pH 9.25. Alternatively, HRP may oxidize (5OH)-L-Trp rather than the colorimetric substrate being monitored by the spectrophotometric assay. Finally, there may be uncoupling between VioA flavin reoxidation and peroxide formation or between peroxide reduction and oxidation of the colorimetric substrate by HRP.

Evidence for such uncoupling came from the identification of an unexpected product of VioA. As can be seen in Figure 2A, during the oxidation of L-tryptophan by VioA, **4** is produced. Attempts to determine kinetic parameters for CPA formation were unsuccessful, as its production was inconsistent and was not linear over time. To decipher the properties of CPA formation, VioA was incubated with [$^{14}C$]-

L-Trp anaerobically, which results in a single turnover reaction because there is no oxygen to regenerate oxidized FAD. As can be seen in Figure 2B, when VioA is used to oxidize L-Trp anaerobically, quenched with acid, and the reaction is immediately injected for HPLC analysis, no CPA is formed. However, if the quenched anaerobic reaction is allowed to sit aerobically for 2 h, CPA is produced. This demonstrates that VioA is not directly responsible for CPA formation. Rather, the reduced flavin reacting with molecular oxygen may generate radicals that spontaneously form CPA from IPA imine, thus explaining its inconsistency and kinetic incompetence.

*Purification of VioB and Identification of VioE.* Very little is understood about the formation of the pyrrolidone core of violacein. It is proposed to be formed by the action of a single enzyme VioB (*6*). This enzyme would have to carry out five chemical transformations: an oxidative carbon−carbon bond formation, an indole shift, two decarboxylations, and a four-electron oxidation to install a ketone. Its closest characterized homologues, RebD (*36*, *49*) and StaD (*50*), carry out only one of these transformations, the oxidative carbon−carbon bond formation. To investigate pyrrolidone formation, VioB was cloned as the C-terminal $His_6$-tagged protein and expressed in *E. coli* at 15 °C, yielding 10 mg/L of protein. The 111 kDa protein was purified to homogeneity using nickel-affinity chromatography and gel filtration in tandem (Figure 1B). VioB purified with heme and non-heme iron cofactors, the content of which differed depending on expression and purification conditions. Native VioB (without in vitro or in vivo reconstitution) contained 0.87 equiv of iron as determined by the Ferene S spectrophotometric assay (*44*) and 0.11 equiv of heme *b* as determined by the pyridine hemochrome UV−vis spectrophotometric assay (*43*). If in vitro reconstitution with hematin was performed, VioB was found to contain 0.76 equiv of iron and 0.47 equiv of hematin. Unfortunately, in both cases, no activity was observed for VioB when incubated with L-tryptophan and VioA. If however VioB was expressed in media supplemented with the heme precursor *δ*-aminolevulinic acid and ammonium iron sulfate, VioB was found to be active, containing 0.84 equiv of iron and 0.31 equiv of heme *b*. It is possible that the excess iron is nonspecifically bound to the $His_6$ tag.

When purified VioB was initially found to be inactive, we wanted to determine whether VioB was active at all in vivo when expressed in the BL21 (DE3) cells used for protein overproduction and whether any additional factors, protein or chemical, may be required for violacein production. The violacein gene clusters, as they have been isolated and previously expressed in heterologous hosts, have contained DNA with genes from regions adjacent to the cluster (*30*−*32*, *40*). Using the restriction enzymes *Mlu*I and *Xho*I, the annotated violacein cluster, and approximately 1000 base pairs of DNA on either side of the cluster, was excised from the genomic DNA of *C. violaceum* and ligated into pET24b. This construct lacks the T7 promoter normally present on the vector, and consequently, transcription of the genes is controlled by the endogenous promoters from *C. violaceum*. Transformation of this vector (pVio) into Top10 or BL21 cells resulted in production of the violacein pigment and purple-colored bacteria.

With VioB activity confirmed, we searched for additional genes that may be involved in violacein production. Using restriction enzymes to create seven deletions within the isolated cluster, we assayed for a loss or change in pigment of the bacteria. As had been previously reported (*30*−*32*), disruption of either VioA or VioB (pVioΔ*Nco*I, pVioΔ*Bgl*II, pVioΔ*Pml*I, pVioΔ*EcoR*I, and pVioΔ*Stu*I) led to complete loss of pigment production (Figure 3A). Deletion of both VioC and VioD (pVioΔ*BstB*I) led to formation of a green pigment in Top10 cells (Figure 3A). When isolated, this pigment was identified as **9** (Scheme 2) by mass spectrometry, UV−vis spectrum, and NMR. Interestingly, when this same construct was transformed into BL21 cells, purple pigment was produced, and upon extraction several compounds were found, including deoxychromoviridans, prodeoxyviolacein, and various other two- and four-electron oxidized versions of prodeoxyviolacein. This would suggest that either the *E. coli* B strain from which BL21 cells are derived contains hydroxylases that recognize the prodeoxyviolacein skeleton that are not present in the *E. coli* K strain from which Top10 cells are derived or that BL21 cells contain a more oxidizing environment in which the electron-rich violacein precursors can react by an autoxidative process. The final deletion (pVioΔ*Bbv*CI) gave a most unanticipated result. Although all four annotated violacein genes were still intact, no pigment was produced (Figure 3A). This deletion removed a small ORF (CV3270) of unknown function that lies directly downstream of VioD.

To confirm these results, the boundaries of the violacein gene cluster were determined by excising the cluster with various lengths of the flanking DNA regions removed, and ligating into pETBlue-2, which contains a broader range multiple cloning site. As can be seen in Figure 3B, deletion of most of the flanking region around the violacein cluster has no effect on pigment production (pVio2-*Mlu*I/*Xho*I, pVio2-*Sbf*I/*Xho*I, pVio2-*Mlu*I/*Asc*I, and pVio2-*Sbf*I/*Asc*I); however, if any of the CV3270 ORF (henceforth known as VioE) is deleted (pVio2-*Mlu*I/*Aat*II and pVio2-*Sbf*I/*Aat*II), pigment production is completely abrogated. To demonstrate that VioE is in fact a transcribed protein involved in violacein production and that there was not simply a polar effect on the violacein cluster from deleting a downstream segment of DNA, complementation experiments were carried out to rescue violacein production. When either the full VioE deletion plasmid (pVio21Δ*BstB*I) or the VioE truncated plasmids (pVio21-*Mlu*I/*Aat*II and pVio21-*Sbf*I/*Aat*II) were cotransformed with stand alone VioE cloned as a C-terminal $His_6$-tagged construct (pVioE), pigment production was restored (Figure 3C). Thus, VioE is a fifth protein essential for violacein production and acts in the early stages of pigment production. After the completion of the studies in Figure 3A−C, J. Salas and co-workers published on the necessity for VioE in heterologous in vivo experiments of the violacein gene cluster in *E. coli* and *Symphoricarpos albus* (*40*), independently validating our results.

*Characterization of VioB and VioE − Formation of Prodeoxyviolacein.* VioE was cloned as the C-terminal $His_6$-tagged protein and expressed in *E. coli* at 25 °C, yielding 25 mg/L of protein. The 22 kDa protein was purified to homogeneity using nickel-affinity chromatography and gel filtration in tandem (Figure 1B). VioE purified with no visible

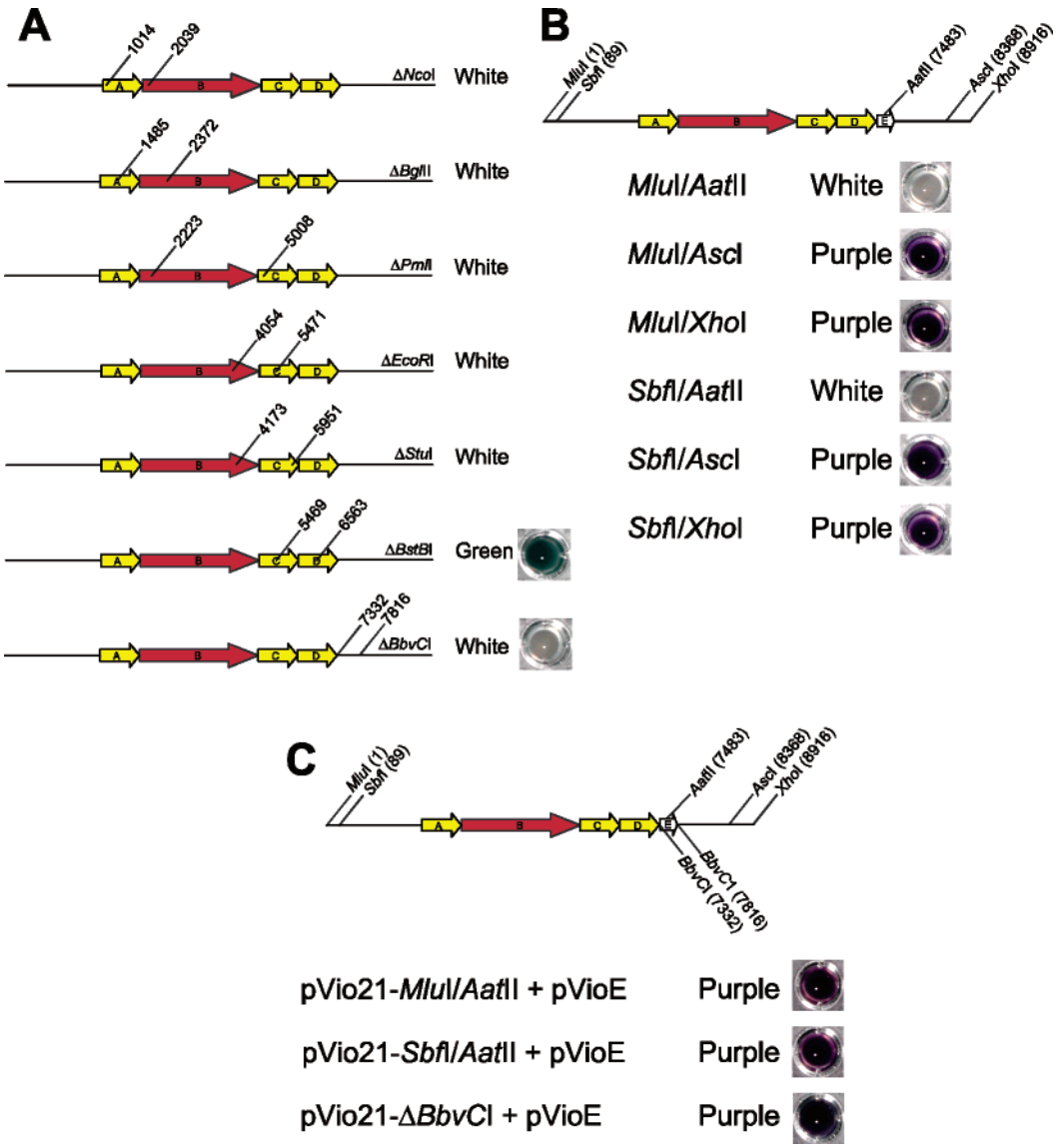


FIGURE 3: (A) Seven deletion mutants of the pVio plasmid using the noted restriction enzyme with the boundaries of the deletion marked. The color of the resulting Top10 *E. coli* culture is stated for all constructs and shown for the pVioΔ*Bst*BI and pVioΔ*Bbv*CI plasmids. (B) The boundaries of the violacein cluster were tested by trimming DNA adjacent to the violacein gene cluster using the noted restriction enzymes to generate six pVio2 constructs. The colors of the resulting Top10 *E. coli* cultures after transformation is stated and shown for all plasmids. (C) Complementation for VioE disruption was carried out by cotransformation of the plasmids pVio21Δ*Bst*BI, pVio21-*Mlu*I/*Aat*II, and pVio21-*Sbf*I/*Aat*II with pVioE in BL21 (DE3) cells. The colors of the resulting *E. coli* cultures is stated and shown for all experiments. The color of the violacein genes denotes cofactor bound to the translated protein, with yellow for FAD and red for heme.

bound cofactors, and ICPMS analysis did not reveal the presence of any bound metals.

On the basis of our in vivo work, it was probable that VioA, VioB, and VioE are all intimately involved in the formation of the pyrrolidone core. We performed incubations with all three proteins as a three-component system to determine whether these enzymes were sufficient for synthesis of prodeoxyviolacein. As can be seen in Figure 4A, incubation of VioA, VioB, VioE, and L-tryptophan led to linear formation of **5** over time. Omission of any three of these proteins or L-tryptophan resulted in no prodeoxyviolacein production (data not shown). It is interesting to note that although conversion to prodeoxyviolacein is complete within 1 h, if the reaction is allowed to proceed for several hours **9** forms (Figure 4A).

Several conditions were tested to optimize production of this key intermediate for violacein. Using an end point assay, the optimum pH for the three enzyme system was determined to be between 9 and 9.5, the same as was observed for L-Trp oxidation by VioA alone (data not shown). Furthermore, addition of catalase greatly improved the rate of product formation. The necessity for catalase was somewhat unexpected because VioB, like RebD, has catalase activity, as determined by its ability to generate oxygen from hydrogen peroxide (data not shown). It is possible that VioB is too slow or has too high a $K_M$ to be effective at disproportionating hydrogen peroxide generated during the catalytic cycle of VioA-mediated oxidation of L-tryptophan. Alternatively, catalase activity at the heme active site of VioB may detract from its role in catalyzing formation of the pyrrolidone core. The need for catalase is not due to inhibition of the reaction by hydrogen peroxide because addition of up to 50 mM hydrogen peroxide in the absence of catalase does not affect product formation (data not shown). Rather, it is the

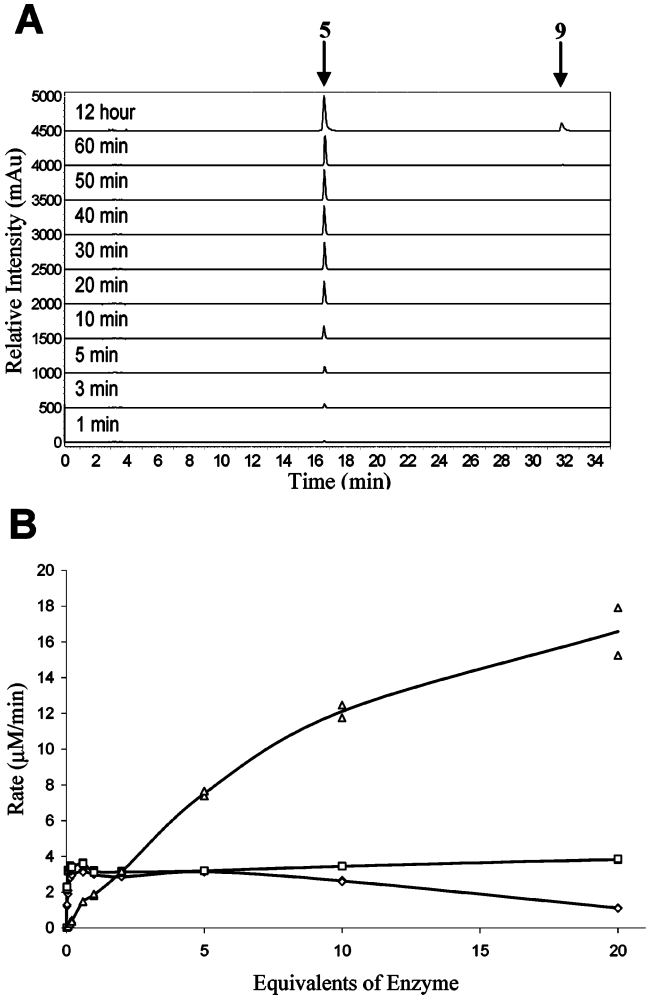


FIGURE 4: (A) Time course for prodeoxyviolacein (**5**) formation from L-Trp (500 $\mu$M) by the action of VioA, VioB, and VioE (5 $\mu$M each). Product formation was monitored at 590 nm. (B) Change in rate of **5** formation at different concentrations of VioA, VioB, or VioE, while keeping the other two enzymes constant at 5 $\mu$M. Diamonds denote changing VioA concentration, triangles denote changing VioB concentration, and squares denote changing VioE concentration.

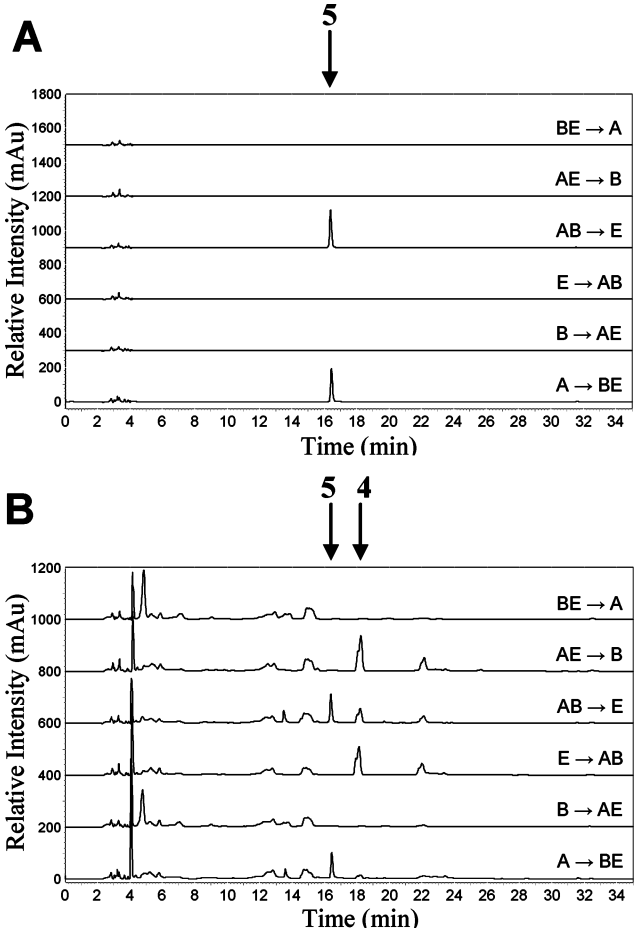


FIGURE 5: (A) Order of action of VioA, VioB, and VioE on route to prodeoxyviolacein (**5**) formation from L-Trp was tested by incubating 5 $\mu$M of one or two of the proteins (letter(s) to the left of the arrow) with 500 $\mu$M L-Trp for 10 min, passing the soluble molecule portion through a 10 kDa filter (signified by the arrow), and reacting with 5 $\mu$M of the remaining protein(s) of the three (letter to the right of the arrow). Product formation was monitored at 590 nm. (B) Same as in A, but monitoring at 280 nm.

dependence of the reaction on molecular oxygen that creates the need for catalase. If the reaction solution is preincubated with hydrogen peroxide and catalase to saturate with oxygen, the final amount of product formed from L-tryptophan by the action of VioA, VioB, and VioE increases greatly (data not shown). Thus, in the presence of VioA, which has been shown to have a fast catalytic cycle, the reaction solution may be depleted of molecular oxygen necessary for efficient formation of prodeoxyviolacein. The intimate correlation between oxygenation and violacein production has been described previously (*24*).

The rate of **5** formation by this three-component system at 5 $\mu$M of each enzyme was determined to be 0.6 min$^{-1}$. To understand which enzyme is rate limiting in the system, the concentration of each enzyme was varied while keeping the others constant. As can be seen in Figure 4B, at concentrations above 300 nM the rate of formation of prodeoxyviolacein does not increase with more VioA or VioE, and in fact decreases at concentrations of VioA above 25 $\mu$M, presumably due to instability of the IPA imine generated. However, the rate of prodeoxyviolacein production increases linearly with increasing amounts of VioB, indicating that VioB catalysis is the rate-limiting step in prodeoxyviolacein production.

Once the minimal system for prodeoxyviolacein production was established, we sought to determine the individual steps catalyzed by these enzymes. First, we wanted to understand the order in which the enzymes act and determine whether there were any necessary protein−protein interactions between VioA, VioB, and VioE. To address these questions, L-tryptophan was incubated with one or a pair of the three enzymes in the system for 10 min, the soluble molecule fraction was passed through a 10 kDa filter to remove the proteins, and the final enzyme or pair of enzymes was added for an additional hour. As can be seen in Figure 5A prodeoxyviolacein was formed only when L-tryptophan was reacted first with VioA or VioA and VioB, and then the intermediate product was shuttled to either VioB and VioE or just VioE, respectively. This demonstrates that there are no required protein−protein interactions and that the order of reaction is VioA, then VioB, and finally VioE.

During these sets of experiments, it was observed that when VioA and VioB were incubated in what was effectively the absence of VioE − either VioA and VioB for 10 min before shuttling to VioE, VioE first before shuttling to VioA

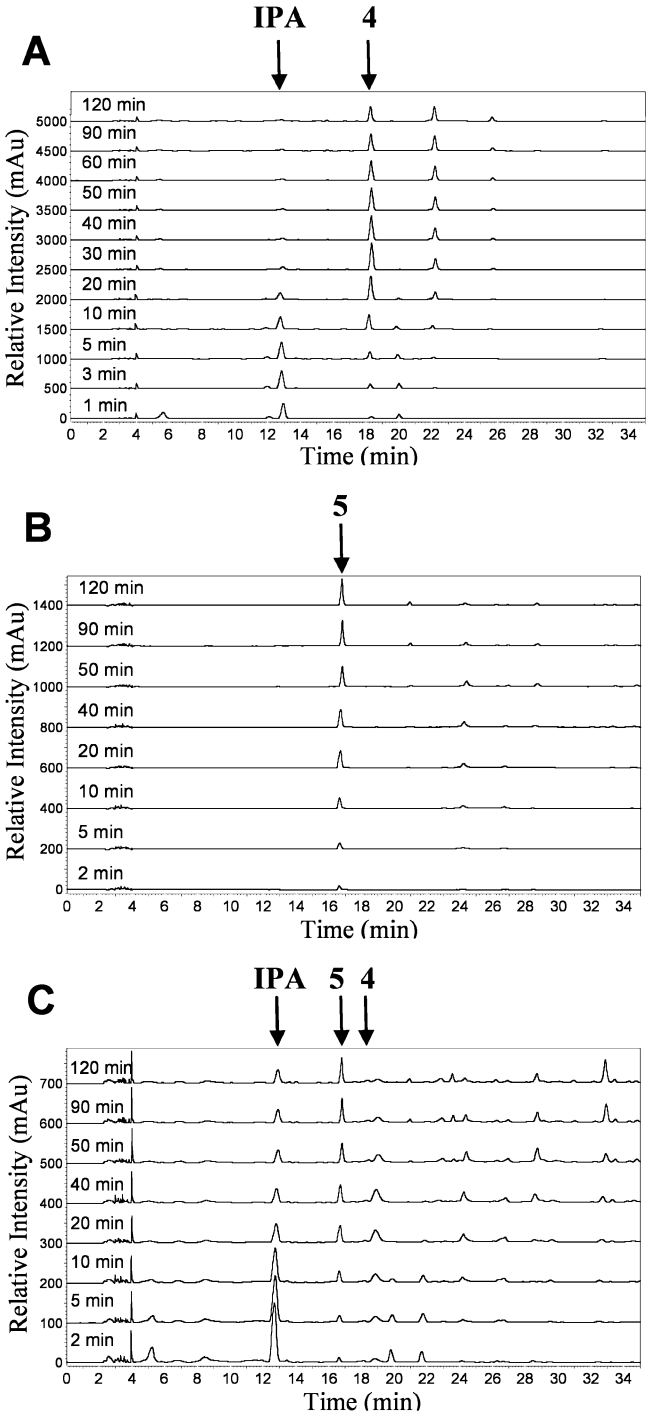


FIGURE 6: (A) Time course of CPA (**4**) formation from L-Trp (500 $\mu$M) by VioA and VioB (5 $\mu$M each), in the absence of VioE. Product was monitored at 280 nm. (B) Time course of prodeoxyviolacein (**5**) formation from L-Trp (500 $\mu$M) by action of RebD (5 $\mu$M) in the presence of VioA (5 $\mu$M) and VioE (5 $\mu$M). Product was monitored at 590 nm. (C) Same as B, but monitoring at 280 nm.

and VioB, or VioA and VioE before shuttling to VioB − CPA was formed (Figure 5B). This led us to suspect that the product of VioA and VioB is the same as RebO and RebD in the rebeccamycin system and this compound is CPA or is a precursor to it. As can be seen in Figure 6A, incubation of L-tryptophan with VioA and VioB produces CPA linearly over time. In this instance, CPA formation is enzyme dependent and is kinetically competent. The peak at 13 min is actually derived from IPA imine and can be reproduced by quenching IPA under the same reaction conditions. Thus, its disappearance tracks with the utilization of oxidized tryptophan. The peak at 22.5 min appears to be a methylated version of CPA (+14 mass shift) generated under the quenching conditions of the reaction, and so its formation parallels the formation of CPA.

Given that the product of VioA and VioB appears to be CPA, we tested whether CPA was on pathway to prodeoxyviolacein. Incubation of CPA with VioE alone or VioA, VioB, and VioE together did not yield prodeoxyviolacein (data not shown). Thus, since CPA is not on pathway to prodeoxyviolacein formation, VioE must reroute an intermediate produced by the tandem action of VioA and VioB to prodeoxyviolacein that would otherwise spontaneously form CPA. To test this and to demonstrate that VioA and VioB mirror RebO and RebD from the rebeccamycin system, VioB was replaced with RebD in the three-component in vitro system. As can be seen in Figure 6B, prodeoxyviolacein is formed. Interestingly, VioE appears to be so efficient that no CPA is formed by RebD (Figure 6C), which is normally on pathway product for the rebeccamycin system. Thus, VioB appears to be a direct homologue of RebD, StaD, and InkD from the indolocarbazole biosynthetic systems and the key difference is VioE, which directs an intermediate, designated **X** in Scheme 1, to formation of prodeoxyviolacein rather than CPA.

*Purification and Characterization of VioC and VioD.* With production of prodeoxyviolacein reconstituted, we decided to investigate the final stages of violacein biosynthesis, which entail two oxygenations. Previously, we did not observe activity of VioD toward L-Trp, so we wanted to test its ability to hydroxylate prodeoxyviolacein at the 5-position of the shifted indole. Additionally, we wanted to test the activity and specificity of VioC, the monooxygenase proposed to hydroxylate the 2-position of the non-shifted indole. VioC was cloned as the C-terminal $His_6$-tagged protein and expressed in *E. coli* at 15 °C, yielding approximately 7 mg/L of protein. The 48 kDa VioC protein was purified to homogeneity using nickel-affinity chromatography and gel filtration in tandem (Figure 1B). VioC purified with an FAD bound cofactor, as determined by analytical HPLC using authentic standards (data not shown). Using UV−vis spectroscopy, the FAD occupancy was determined to be 9% before reconstitution and 43% after in vitro reconstitution.

VioC and VioD were tested for their ability to hydroxylate **5** by directly using reducing equivalents of NAD(P)H. As can be seen in Figure 7A, VioC is able to generate **7** using either NADPH or NADH and VioD is able to generate proviolacein (**6**) using either NADPH or NADH. Incubation of prodeoxyviolacein with VioC, VioD, and NAD(P)H yielded fully oxidized **8**. To determine whether VioC and VioD would recognize the reciprocal two-electron reduced precursors of violacein, prodeoxyviolacein was incubated for 2 h with one of the hydroxylases to allow for complete conversion to either proviolacein or deoxyviolacein and then the second hydroxylase, VioC or VioD, respectively, was added. It was determined that VioC will hydroxylate proviolacein; however, VioD will not hydroxylate deoxyviolacein (Figure 7B). The very small peak of deoxyviolacein at 14 min and violacein at 19 min in the reaction of VioD with deoxyviolacein is derived from VioD hydroxylating unreacted prodeoxyviolacein that had not been fully turned

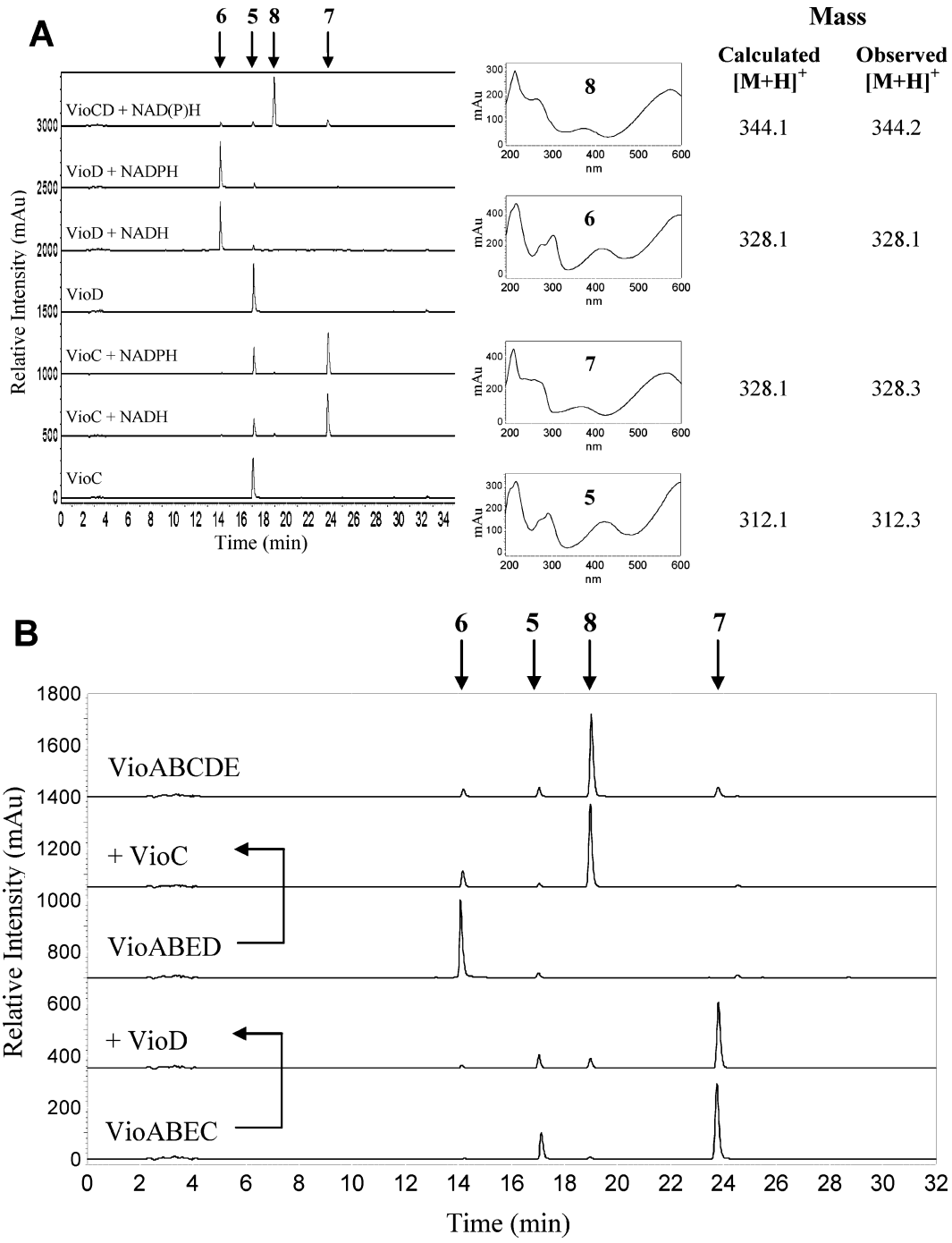


FIGURE 7: (A) Action of 5 $\mu$M VioC and/or VioD on prodeoxyviolacein (**5**) in the presence or absence of 5 $\mu$M NAD(P)H. Reactions are monitored at 590 nm. UV−vis spectra and masses for reactants and products are included. (B) Action of 5 $\mu$M VioC on proviolacein (**6**) (formed by incubation of 500 $\mu$M L-Trp with 5 $\mu$M VioABED and 5 $\mu$M NADPH) and of 5 $\mu$M VioD on deoxyviolacein (**7**) (formed by incubation of 500 $\mu$M L-Trp with 5 $\mu$M VioABEC and 5 $\mu$M NADPH) Coincubation of 500 $\mu$M L-Trp with 5 $\mu$M VioABCDE and 5 $\mu$M NADPH to generate violacein (**8**) is included for reference. All reactions are monitored at 590 nm.

over by VioC. Thus, the order of hydroxylation on route to violacein is VioD followed by VioC (Scheme 1).

## DISCUSSION

**8** represents a unique bisindolepyrrolidone natural product with a wide range of biological activities (*7*−*22*). Derived from two molecules of L-tryptophan, violacein undergoes a 14-electron oxidation process in its generation (*3*, *4*, *6*, *24*). Both in structure and biosynthetic machinery violacein is most similar to the indolocarbazole class of natural products (*30*−*35*). Although violacein has been known since 1882 (*5*), little is known about the chemical transformations leading to its generation. Genetic work had only led to the functional assignment of two flavin dependent hydroxylases (*6*, *30*); however, questions still persist about the order in which they act, as well as their substrate specificities. The most unique transformation, formation of the pyrrolidone core with a 1,2-shift of indole on one side (*4*, *26*), remained essentially uncharacterized.

We have recently described the in vitro reconstitution of chromopyrrolic acid (CPA) (**4**) formation, an intermediate on pathway to **1** and **2**, using the amino acid oxidase RebO

Scheme 1: Overall Pathway to Violacein Biosynthesis

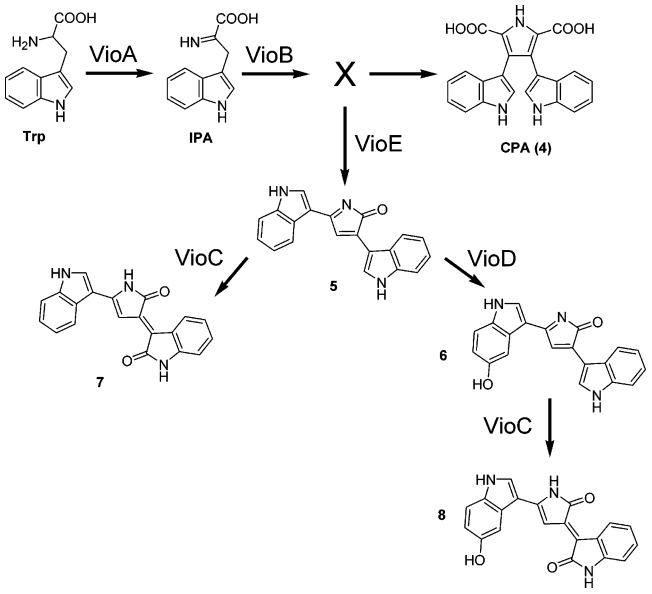


(*51*) and hemoprotein oxidase RebD (*36*). These two proteins parallel the early biosynthetic enzymes VioA and VioB in the violacein pathway. Like RebO, we have shown that VioA is an FAD dependent L-Trp amino acid oxidase which generates the IPA imine. VioB, a unique protein that shares 36% identity to StaD, 34% identity to RebD, 45% identity to InkD, and 38% identity to AtD—all CPA synthases involved in indolocarbazole formation—too is a hemoprotein oxidase. In the absence of any other proteins, we have demonstrated that tandem incubations of VioA and VioB yield robust formation of CPA, just like RebO and RebD. Furthermore, like RebD, VioB has catalase activity. As with RebD, it is proposed that the heme iron center and not the non-heme iron center is responsible for catalysis.

One difference is that unlike RebD, VioB is unable to form CPA from IPA and ammonium ions (data not shown). However, this may be explained by the pH in which the reaction occurs. It has been shown that the preferred substrate for RebD is two molecules of the IPA imine (*36*). Formation of the IPA imine from IPA ketone and ammonium is favored at lower pH due to the need to protonate the ketone during the exchange reaction. Since the optimal pH for the violacein enzymes is 9.25, almost two units above the optimal pH for the rebeccamycin enzymes, the exchange reaction to generate IPA imine may not be robust enough to facilitate catalysis by VioB. Another key difference between VioB and RebD is the heme occupancy of the enzyme. RebD has been shown to contain between 1.3 and 1.8 equiv of heme after reconstitution (*36*). However, VioB is active with 31% heme occupancy and reconstitution in the same manner as performed for RebD only leads to 47% heme occupancy. Since both enzymes appear to carry out the same enzymatic reaction, this would suggest that only a single heme center is catalytic in RebD. As has been previously demonstrated for RebD (*36*), VioB is proposed to utilize $O_2$ at its heme center for the oxidative dimerization of two molecules of IPA imine.

Given that VioA and VioB can also form CPA, it seemed at first odd that CPA is not on the pathway to violacein, as shown by feeding experiments (*37*, *40*), and our in vitro work where CPA was not converted to **5**. Our genetic analysis of the violacein pathway demonstrates the need for a fifth, unannotated gene, *vioE*, which lies immediately downstream from v*ioD* and is transcribed in the same direction as the other four biosynthetic enzymes. Although VioE has no known homologues, it is present in the violacein clusters from various strains of *C. violaceum* (*30*, *32*) as well as a proposed violacein cluster from *Pseudoalteromonas tunicate* D2, which is known to produce a purple pigment (*52*). Our findings demonstrating the necessity of VioE independently confirm those reported in a very recent paper from the Salas laboratory (*40*). Tandem incubation of pure VioE with VioA and VioB does in fact produce prodeoxyviolacein, with no CPA formation. Thus, VioE must be responsible for the 1,2-shift of the indole substituent on route to prodeoxyviolacein.

To understand whether VioE operates on a soluble intermediate or whether it is involved in some protein−protein interaction that redirects the enzymatic reaction carried out by VioB, we performed a series of reactions in which soluble intermediates from one or a pair of the VioA, VioB, and VioE enzymes were separated from the first enzymes and shuttled to the remaining single or pair of enzymes. We were able to demonstrate that there are no necessary protein−protein interactions between this three-component system and that the order of reaction is VioA, then VioB, and finally VioE. This establishes that the actual product synthesized by VioA and VioB is not CPA, but rather a molecule, designated **X** in Scheme 1, that spontaneously forms CPA unless otherwise rerouted by VioE. We were also able to show that VioB and RebD are interchangeable and that in the presence of VioE, RebD no longer forms CPA, but instead the only product is prodeoxyviolacein. This validates that VioB and RebD are indeed true homologues, carry out the same chemical reaction, and release a diffusible nascent product that can be rerouted by VioE.

The identity of the intermediate compound formed by the action of VioA and VioB (or RebO and RebD) is not yet known, but it can be converted to prodeoxyviolacein and must still contain both carboxylates and an unshifted indole, due to its spontaneous conversion to CPA. It has previously been proposed that the RebOD reaction proceeds by initial formation of a condensation product between an IPA imine and its corresponding enamine tautomer to yield a cross coupled imine (*36*). However, if RebD and VioB are responsible for the oxidative coupling between the two benzylic $\beta$-carbons of L-Trp, this cannot be the intermediate, because it would lead to direct formation of CPA, which does not convert to prodeoxyviolacein. Instead, it is more likely that VioB and RebD catalyze benzylic carbon−carbon coupling of two molecules of IPA to yield proposed molecule **X** with two imines (Scheme 2). As shown on the right-hand side of Scheme 2, compound **X** can tautomerize and spontaneously undergo intramolecular condensation to form CPA. Alternatively, it is intercepted by VioE. The observed net 1,2-shift of the indole might occur by the indicated cyclopropane species, set up for decarboxylation, cyclization, loss of ammonia, and loss of the second carboxylate. This path still requires a subsequent four-electron oxidation to install the ketone of the pyrrolidone and generate prodeoxyviolacein, the accumulating product from incubations of VioABE, a process that may proceed via autoxidation (Scheme 2). Although it is tempting to propose that the 1,2

Scheme 2: Possible Mechanism for VioE-Mediated Divergence of Prodeoxyviolacein (**5**) from Chromopyrrolic Acid (CPA) (**4**)

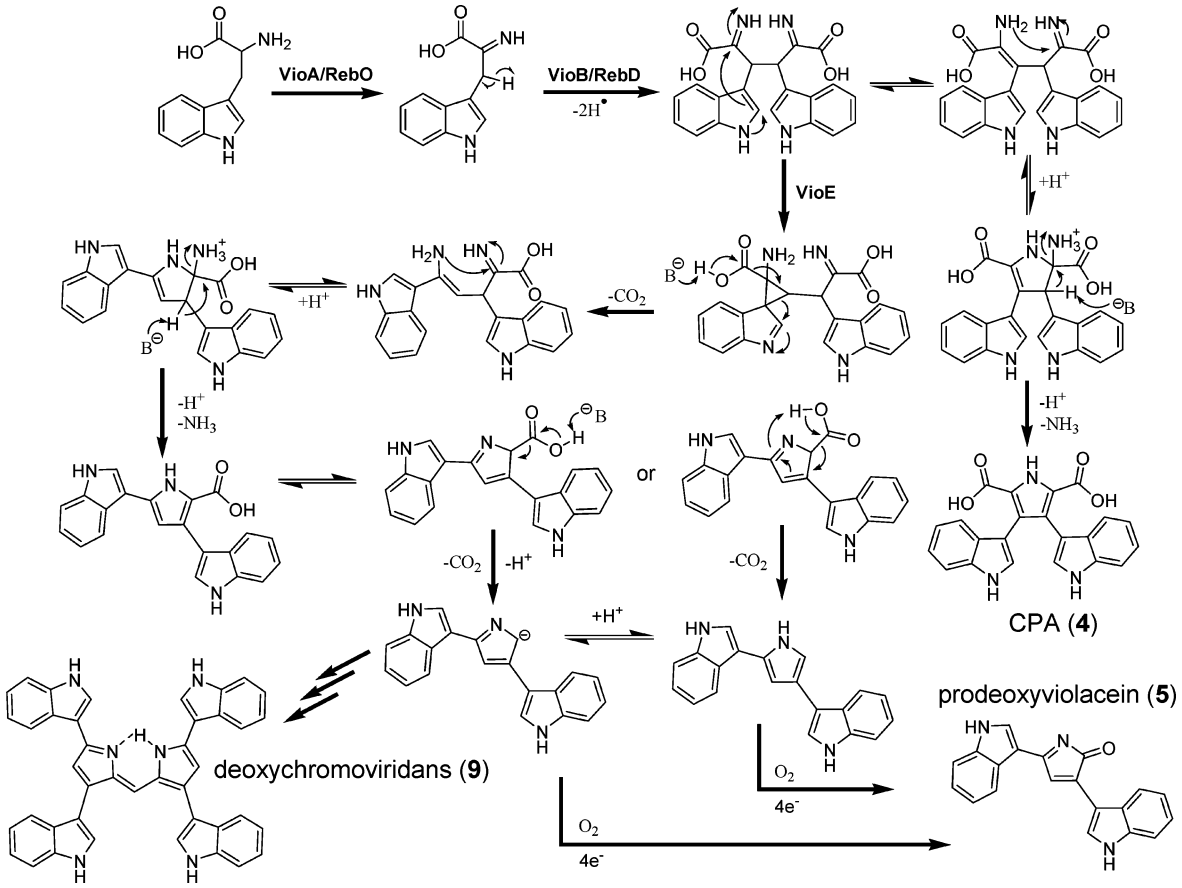


indole shift occurs via a radical-mediated mechanism as with other previously reported 1,2 shifts (*27*−*29*), the fact that VioE contains no cofactors, metal or otherwise, and operates on an intermediate that is stable in solution for at least 10 min, would seem to rule out radical formation and leaves us to propose the aforementioned mechanism or a stepwise variant of it.

Given that the intermediates on the way to production of prodeoxyviolacein are so unstable it is surprising that no protein−protein interactions are necessary to shield reactive intermediates from nonproductive reactions. The IPA imine is readily hydrolyzed in solution to form the ketone and its less predominant enol tautomer. Furthermore, IPA itself is unstable in solution and degrades to various oxidative byproducts. Additionally, the nascent product (**X**) of VioA and VioB obviously forms CPA spontaneously, although CPA is not on the pathway to prodeoxyviolacein formation. A similar situation is observed in the rebeccamycin system where no evidence for a complex between RebO and RebD is observed (*36*). Obviously, there is a coupled and rapid reaction between RebO/RebD and VioA/VioB/VioE that is effective at shepherding intermediates down the biosynthetic chain toward more stable products. Future work will be directed toward elucidation of the structure of the nascent product, **X**, from RebOD and VioAB.

In our initial assays demonstrating tryptophan oxidation to IPA by VioA, we found that CPA could be formed in the absence of VioB. CPA formation under these conditions was found to be dependent on oxygen but independent of VioA once IPA was formed. Because of the inconsistency of this reaction and its kinetic incompetence, we propose that CPA is being formed spontaneously by radicals generated from $O_2$ and reduced flavin. Given our proposed mechanism of CPA formation from intermediate **X** (Scheme 2), should a radical be generated at the benzylic $\beta$-carbon of IPA, carbon−carbon bond formation could occur, after which formation of CPA would be spontaneous. It is obvious that this route to CPA formation is not the major one given that VioB is required for violacein production and RebD is required for CPA production in vivo and that VioB and RebD yield a catalytically competent reaction with tremendously improved turnover rates and consistency in vitro.

During our investigation into the production of prodeoxyviolacein, we observed that prolonged incubations of VioA, VioB, and VioE with L-tryptophan actually resulted in production of the dimeric **9**. Previous in vivo work had demonstrated that the extra methenyl carbon bridging the dimer was derived from serine and that supplementation with tetrahydrofolate (THF) increased the production of deoxychromoviridans (*48*). This suggested the involvement of serine hydroxymethyltransferase and generation of $N^5$,$N^{10}$-methylene THF to create a reactive methylating agent responsible for bridging two molecules of prodeoxyviolacein. However, here the Vio enzymes are able to form deoxychromoviridans without the need for THF or serine. It is not yet known from where the methenyl carbon is derived.

There was an outstanding question as to whether VioD acts in the first steps of violacein biosynthesis to generate 5OH-L-tryptophan which is taken through to generate the pyrrolidone core, or whether hydroxylation occurs later in biosynthesis. There are contradicting reports as to whether 5OH-L-Trp is a viable precursor that can be incorporated

into violacein when fed to *C. violaceum* (*3*, *6*, *39*). In rebeccamycin formation, a related indolocarbazole, it has been shown that RebH, a flavin halogenase, acts to generate 7Cl-L-Trp (*53*, *54*) before amino acid oxidation and subsequent oxidative dimerization to 1,11-dichlorochromopyrrolic acid by tandem action of RebO and RebD, respectively (*36*). Although RebO is capable of oxidizing just L-Trp with subsequent dimerization to CPA by RebD, kinetic parameters demonstrate that 7Cl-L-Trp is the better substrate (*51*).

Here we reconstituted the activity of purified VioC and VioD. Both were determined to be single-component FAD-dependent monooxygenases that could use either NADH or NADPH as reducing equivalents in their catalytic cycle. VioD does not hydroxylate L-tryptophan but instead works at late stages in violacein biosynthesis, hydroxylating **5**. VioC will hydroxylate both prodeoxyviolacein and **6**. **7** is not a substrate for VioD, and thus the order of oxidation must be hydroxylation of prodeoxyviolacein by VioD, followed by hydroxylation of proviolacein by VioC to form **8** (Scheme 1). The production of deoxyviolacein in vivo represents a deviation in the order of hydroxylation, where VioC acts before VioD, generating a product that is not recognized by VioD.

In reconstituting the biosynthetic pathway to violacein, via heterologous expression and in vitro characterization of VioA, VioB, VioC, VioD, and VioE, we have unambiguously demonstrated the overall biosynthetic route to this intriguing natural product. VioA and VioB have been shown to be direct homologues to the CPA forming enzymes in the indolocarbazole biosynthetic pathways, with the unique VioE protein representing the sole factor controlling formation of prodeoxyviolacein versus CPA. Furthermore, it was demonstrated that CPA is not the actual product of VioB/RebD, but rather an unstable compound that spontaneously forms CPA is synthesized. VioB represents the third characterized member (*36*, *49*, *50*) of a unique hemoprotein family that does not require an exogenous electron shuttling cofactor to carry out a two-electron oxidative coupling of two molecules of IPA imine. Finally, we have explained why both violacein and deoxyviolacein are produced naturally in vivo in *C. violaceum.*

## ACKNOWLEDGMENT

We thank Dr. Annaleise Howard-Jones for the gift of chromopyrrolic acid standard, RebD enzyme, and a careful reading of the manuscript.

## REFERENCES

1. Moreau, P., Anizon, F., Sancelme, M., Prudhomme, M., Bailly, C., Severe, D., Riou, J. F., Fabbro, D., Meyer, T., and Aubertin, A. M. (1999) Syntheses and biological activities of rebeccamycin analogues. Introduction of a halogenoacetyl substituent, *J. Med. Chem. 42*, 584−592.
2. Tamaoki, T., Nomoto, H., Takahashi, I., Kato, Y., Morimoto, M., and Tomita, F. (1986) Staurosporine, a potent inhibitor of phospholipid/$Ca^{++}$dependent protein kinase, *Biochem. Biophys. Res. Commun. 135*, 397−402.
3. Demoss, R. D., and Evans, N. R. (1960) Incorporation of C14-labeled substrates into violacein, *J. Bacteriol. 79*, 729−733.
4. Hoshino, T., Kondo, T., Uchiyama, T., and Ogasawara, N. (1987) Biosynthesis of violacein: a novel rearrangement in tryptophan metabolism with a 1,2-shift of the inodle ring, *Agric. Biol. Chem. 51*, 965−968.
5. Boisbaudran, L. D. (1882) Matiere colarante se formant dans la cole de farine, *Compt. Rend. 94*, 562.
6. Antonio, R. V., and Creczynski-Pasa, T. B. (2004) Genetic analysis of violacein biosynthesis by *Chromobacterium violaceum*, *Genet. Mol. Res. 3*, 85−91.
7. Duran, N., Erazo, S., and Campos, V. (1983) Bacterial chemistry-II: antimicrobial photoproduct from pigment of *Chromobacterium violaceum*, *An. Acad. Bras. Cienc. 55*, 231−234.
8. Duran, N., and Menck, C. F. (2001) Chromobacterium violaceum: a review of pharmacological and industiral perspectives, *Crit. Rev. Microbiol. 27*, 201−222.
9. Lichstein, H. C., and Van de Sand, V. F. (1945) Violacein, an antibiotic pigment produced by *Chromobacterium violaceum*, *J. Infect. Dis. 76*, 47−51.
10. Andrighetti-Frohner, C. R., Antonio, R. V., Creczynski-Pasa, T. B., Barardi, C. R., and Simoes, C. M. (2003) Cytotoxicity and potential antiviral evaluation of violacein produced by *Chromobacterium violaceum*, *Mem. Inst. Oswaldo Cruz 98*, 843−848.
11. May, G., Brummer, B., and Ott, H. Treatment of prophylaxis of polio and herpes virus infections comprises admin. of 3-(1,2-dihydro-5-(5-hydroxy-1H-indol-3-yl)-2-oxo-3H-pyrrole-3-ylidene)-1,3-dihydro-2H-indol-2-one. Ger OffenDE 3935066, 25 April, 1991.
12. de Carvalho, D. D., Costa, F. T., Duran, N., and Haun, M. (2006) Cytotoxic activity of violacein in human colon cancer cells, *Toxicol. In Vitro*.
13. Kodach, L. L., Bos, C. L., Duran, N., Peppelenbosch, M. P., Ferreira, C. V., and Hardwick, J. C. (2006) Violacein synergistically increases 5-fluorouracil cytotoxicity, induces apoptosis and inhibits Akt-mediated signal transduction in human colorectal cancer cells, *Carcinogenesis 27*, 508−516.
14. Melo, P. S., Justo, G. Z., de Azevedo, M. B., Duran, N., and Haun, M. (2003) Violacein and its beta-cyclodextrin complexes induce apoptosis and differentiation in HL60 cells, *Toxicology 186*, 217−225.
15. Melo, P. S., Maria, S. S., Vidal, B. C., Haun, M., and Duran, N. (2000) Violacein cytotoxicity and induction of apoptosis in V79 cells, *In Vitro Cell Dev. Biol. Anim. 36*, 539−543.
16. Saraiva, V. S., Marshall, J. C., Cools-Lartigue, J., and Burnier, M. N., Jr. (2004) Cytotoxic effects of violacein in human uveal melanoma cell lines, *Melanoma Res. 14*, 421−424.
17. Ferreira, C. V., Bos, C. L., Versteeg, H. H., Justo, G. Z., Duran, N., and Peppelenbosch, M. P. (2004) Molecular mechanism of violacein-mediated human leukemia cell death, *Blood 104*, 1459−1464.
18. Caldas, L. R., Leitao, A. A. C., Santos, S. M., and Tyrrell, R. M. (1978) In *International Symposium on Current Topics in Radiology and Photobiology* (Tyrrell, R. M., Ed.) pp 121−126, Academia Brasileira de Ciencias, Rio De Janeiro.
19. Duran, N., Antonio, R. V., Haun, M., and Pilli, R. A. (1994) Biosynthesis of a trypanocide by *Chromobacterium violaceum*, *World J. Microbiol. Biotechnol. 10*, 686−690.
20. Duran, N., Campos, V., Riveros, R., Joyas, A., Pereira, M. F., and Haun, M. (1989) Bacterial chemistry-III: preliminary studies on trypanosomal activities of *Chromobacterium violaceum* products, *An. Acad. Bras. Cienc. 61*, 31−36.
21. Leon, L. L., Miranda, C. C., De Souza, A. O., and Duran, N. (2001) Antileishmanial activity of the violacein extracted from *Chromobacterium violaceum*, *J. Antimicrob. Chemother. 48*, 449−450.
22. Duran, N., Justo, G. Z., Melo, P. S., De Azevedo, M. B., Brito, A. R., Almeida, A. B., and Haun, M. (2003) Evaluation of the antiulcerogenic activity of violacein and its modulation by the inclusion complexation with beta-cyclodextrin, *Can. J. Physiol. Pharmacol. 81*, 387−396.
23. Ballantine, J. A., Beer, R. J., Crutchley, D. J., Dodd, G. M., and Palmer, D. R. (1958) The synthesis of violacein and related compounds, *Proc. Chem. Soc. 1*, 232−234.
24. Hoshino, T., Takano, T., Hori, S., and Ogasawara, N. (1987) Biosynthesis of violacein: origins of hydrogen, nitrogen and oxygen atoms in the 2-pyrrolidone nucleus, *Agric. Biol. Chem. 51*, 2733−2741.
25. Walsh, C. T., Garneau-Tsodikova, S., and Howard-Jones, A. R. (2006) Biological formation of pyrroles: nature's logic and enzymatic machinery, *Nat. Prod. Rep. 23*, 517−531.
26. Momen, A. Z., and Hoshino, T. (2000) Biosynthesis of violacein: intact incorporation of the tryptophan molecule on the oxindole side, with intramolecular rearrangement of the indole ring on the 5-hydroxyindole side, *Biosci. Biotechnol. Biochem. 64*, 539−549.

27. Bassan, A., Blomberg, M. R., and Siegbahn, P. E. (2003) Mechanism of aromatic hydroxylation by an activated FeIV═O core in tetrahydrobiopterin-dependent hydroxylases, *Chemistry 9*, 4055−4067.
28. Hashim, M. F., Hakamatsuka, T., Ebizuka, Y., and Sankawa, U. (1990) Reaction mechanism of oxidative rearrangement of flavanone in isoflavone biosynthesis, *FEBS Lett. 271*, 219−222.
29. Li, R., Reed, D. W., Liu, E., Nowak, J., Pelcher, L. E., Page, J. E., and Covello, P. S. (2006) Functional genomic analysis of alkaloid biosynthesis in *Hyoscyamus niger* reveals a cytochrome P450 involved in littorine rearrangement, *Chem. Biol. 13*, 513−520.
30. August, P. R., Grossman, T. H., Minor, C., Draper, M. P., MacNeil, I. A., Pemberton, J. M., Call, K. M., Holt, D., and Osburne, M. S. (2000) Sequence analysis and functional characterization of the violacein biosynthetic pathway from *Chromobacterium violaceum*, *J. Mol. Microbiol. Biotechnol. 2*, 513−519.
31. Brady, S. F., Chao, C. J., Handelsman, J., and Clardy, J. (2001) Cloning and heterologous expression of a natural product biosynthetic gene cluster from eDNA, *Org. Lett. 3*, 1981−1984.
32. Pemberton, J. M., Vincent, K. M., and Penfold, R. J. (1991) Cloning and heterologous expression of the violacein biosynthesis gene cluster from *Chromobacterium violaceum*, *Curr. Microbiol. 22*, 355−358.
33. Onaka, H., Taniguchi, S., Igarashi, Y., and Furumai, T. (2003) Characterization of the biosynthetic gene cluster of rebeccamycin from *Lechevalieria aerocolonigenes* ATCC 39243, *Biosci. Biotechnol. Biochem. 67*, 127−138.
34. Onaka, H., Taniguchi, S., Igarashi, Y., and Furumai, T. (2002) Cloning of the staurosporine biosynthetic gene cluster from Streptomyces sp. TP-A0274 and its heterologous expression in *Streptomyces lividans*, *J. Antibiot. (Tokyo) 55*, 1063−1071.
35. Oh, K. B., Kim, S. Y., Park, J. S., Shin, J.-H., Lee, J. Y. and Chae, C. S. (2006), School of Agriculture Biotechnology, Seoul National University.
36. Howard-Jones, A. R., and Walsh, C. T. (2005) Enzymatic generation of the chromopyrrolic acid scaffold of rebeccamycin by the tandem action of RebO and RebD, *Biochemistry 44*, 15652−15663.
37. Hoshino, T., Kojima, Y., Hayashi, T., Uchiyama, T., and Kaneko, K. (1993) A new metabolite of tryptophan, chromopyrrolic acid, produced by *Chromobacterium violaceum*, *Biosci. Biotech. Biochem. 57*, 775−781.
38. Hoshino, T., Hayashi, T., and Odajima, T. (1995) Biosynthesis of violacein: oxygenation at the 2-position of the indole ring and structures of proviolacein, prodeoxyviolacein and pseudoviolacein, the plausible biosynthetic intermediates of violacein and deoxyviolacein, *J. Chem. Soc. Perkin Trans. 1*, 1565−1571.
39. Hoshino, T., and Ogasawara, N. (1990) Biosynthesis of Violacein: Evidence for the intermediacy of 5-hydroxy-L-tryptophan and the structure of a new pigment, oxyviolacein, produced by the metabolism of 5-hydroxytryptophan, *Agric. Biol. Chem. 54*, 2339−2346.
40. Sanchez, C., Brana, A. F., Mendez, C., and Salas, J. A. (2006) Reevaluation of the violacein biosynthetic pathway and its relationship to indolocarbazole biosynthesis, *Chembiochem 7*, 1231−1240.
41. Sambrook, J., Fritsch, E. F., and Maniatis, T. (1989) *Molecular Cloning: A Laboratory Manual*, 2nd ed., Cold Spring Harbor Press, Painview, NY.
42. Bradford, M. M. (1976) A rapid and sensitive method for the quantitation of microgram quantities of protein utilizing the principle of protein-dye binding, *Anal. Biochem. 72*, 248−254.
43. Berry, E. A., and Trumpower, B. L. (1987) Simultaneous determination of hemes a, b, and c from pyridine hemochrome spectra. *Anal. Biochem. 161*, 1−15.
44. Haigler, B. E., and Gibson, D. T. (1990) Purification and properties of NADH-ferredoxinNAP reductase, a component of naphthalene dioxygenase from Pseudomonas sp. strain NCIB 9816, *J. Bacteriol. 172*, 457−464.
45. Dorrestein, P. C., Yeh, E., Garneau-Tsodikova, S., Kelleher, N. L., and Walsh, C. T. (2005) Dichlorination of a pyrrolyl-S-carrier protein by FADH2-dependent halogenase PltA during pyoluteorin biosynthesis, *Proc. Natl. Acad. Sci. U.S.A. 102*, 13843−13848.
46. Delieu, T., and Walker, D. A. (1972) An improved cathode for the measurement of photosynthetic oxygen evolution by isolated chloroplasts, *New Phytol. 71*, 201−225.
47. Vaillancourt, F. H., Han, S., Fortin, P. D., Bolin, J. T., and Eltis, L. D. (1998) Molecular basis for the stabilization and inhibition of 2, 3-dihydroxybiphenyl 1,2-dioxygenase by *t*-butanol, *J. Biol. Chem. 273*, 34887−34895.
48. Momen, A. Z., Mizuoka, T., and Hoshino, T. (1998) Studies on the biosynthesis of violacein. Part 9. Green pigments possessing tetraindole and dipyrromethene moieties, chromoviridans and deoxychromoviridans, produced by a cell free extract of *Chromobacterium violaceum* and their biosynthetic origins, *J. Chem. Soc., Perkin Trans. 1*, 3087−3092.
49. Nishizawa, T., Gruschow, S., Jayamaha, D. H., Nishizawa-Harada, C., and Sherman, D. H. (2006) Enzymatic assembly of the bisindole core of rebeccamycin, *J. Am. Chem. Soc. 128*, 724−725.
50. Asamizu, S., Kato, Y., Igarashi, Y., Tamotsu, F., and Onaka, H. (2006) Direct formation of chromopyrrolic acid from the indole-3-pyruvic acid by StaD, a novel hemoprotein in indolocarbazole biosynthesis, *Tetrahedron Lett. 47*, 473−475.
51. Nishizawa, T., Aldrich, C. C., and Sherman, D. H. (2005) Molecular analysis of the rebeccamycin -amino acid oxidase from *Lechevalieria aerocolonigenes* ATCC 39243, *J. Bacteriol. 187*, 2084−2092.
52. Egan, S., James, S., Holmstrom, C., and Kjelleberg, S. (2002) Correlation between pigmentation and antifouling compounds produced by *Pseudoalteromonas tunicata*, *Environ. Microbiol. 4*, 433−442.
53. Yeh, E., Cole, L. J., Barr, E. W., Bollinger, J. M., Jr., Ballou, D. P., and Walsh, C. T. (2006) Flavin redox chemistry precedes substrate chlorination during the reaction of the flavin-dependent halogenase RebH, *Biochemistry 45*, 7904−7912.
54. Yeh, E., Garneau, S., and Walsh, C. T. (2005) Robust in vitro activity of RebF and RebH, a two-component reductase/halogenase, generating 7-chlorotryptophan during rebeccamycin biosynthesis, *Proc. Natl. Acad. Sci. U.S.A. 102*, 3960−3965.

BI061998Z